PROCEEDINGS, 48th Workshop on Geothermal Reservoir Engineering
Stanford University, Stanford, California, February 6-8, 2023
SGP-TR-224

Paleothermometry of an Enigmatic Travertine Deposit: Cottonwood Travertine, Stillwater Range, Nevada

Amanda Jackson, Owen A. Callahan, Siti R. Mat, Emma Heitmann, Andrew Schauer, Cassandra Brigham, Jay Mudambi, Jennifer Osako, Emma Sullivan, Katharine Huntington, and Juliet G. Crider

367 Panama St, Room 015 Desk N, Stanford, CA 94305

ajacks@stanford.edu

Keywords: Dixie Valley, clumped isotopes, travertine

ABSTRACT

Hot and cold spring travertine deposits record integrated histories reflecting changing hydrologic conditions, informing our understanding of the driving forces behind factors impacting local hydrology. We present results from a geologic and geochemical investigation of Cottonwood Travertine, located in Dixie Valley, NV, where it is unclear if the paleospring system that deposited the travertine was driven by deeply sourced hydrothermal fluids, or high fluid flow driven by wetter paleoclimate conditions. The temperature of the spring water that precipitated the Cottonwood Travertine has implications for the relative importance of hydrothermal versus climatic processes influencing the formation and cessation of this enigmatic deposit.

We identified four groups of samples based on geologic setting, sample textures, and stable and clumped isotopic analysis: 1) calcite-cemented upper gravels, 2) a mound area at the upper bench of the deposit, 3) samples from the flanks and from vuggy veins and fault zone cements from the base of the deposit, and 4) fibrous sub-travertine veins. The calcite-cemented gravels yielded $\delta^{18}O_C$ values as low as -18.4‰ (VPDB) and apparent $T\Delta_{47}$ of 52°C. The top mound of the deposit returned calcite $\delta^{18}O_C$ values between -12.8‰ and -11.7‰ (VPDB) and clumped isotope temperatures ($T\Delta_{47}$) of 24 – 32°C. Higher $\delta^{13}C$ and $\delta^{18}O_c$ values at the mound site are interpreted to reflect off gassing of CO_2 and disequilibrium conditions. $\delta^{18}O_C$ and $T\Delta_{47}$ values from the slopes and base of the deposit are between -15.9‰ and -14.5‰ (VPDB) and around 20°C, respectively. Structurally, texturally, and isotopically ($\delta^{18}O_C$ = -29.4‰ (VPDB); $T\Delta_{47}$ = 93°C), the fibrous sub-travertine veins are more consistent with the local Jurassic host rock and probably do not reflect recent hot spring conditions. Our analysis suggests that, despite the impressive volume, Cottonwood Travertine formed from springs that were not particularly hot, and the deposit instead reflects vigorous warm spring activity in a wetter climactic regime rather than fluid flow from an extinct higher temperature hydrothermal system.

1. INTRODUCTION

Hot and cold spring travertine deposits record integrated histories reflecting changing hydrologic conditions, from evolving climate to postseismic changes in fluid flow. Describing the evolution of these features thus informs our understanding of the driving forces behind factors impacting local hydrology. Dixie Valley in north central Nevada contains a rich record of significant hydrologic changes following climate fluctuations and numerous active and fossil hydrothermal deposits (Figure 1), thus providing a fantastic venue to compare the impact of climate on hydrothermal discharge. Quaternary climate fluctuations impacting local paleohydrology manifest as approximately coeval changes in shoreline elevations across the western Great Basin, including Lake Dixie (Thompson and Burke, 1973; Caskey and Ramelli, 2004) and Lake Lahontan (e.g. Benson, 1993; Adams et al., 2008). Lake depths and shoreline elevations respond to subtle changes in precipitation and evaporation and have been shown to be responding to major climate fluctuations observed in Greenland ice core records (Lin, 1998). The youngest intervals of lake level fluctuations are well documented, but there is also evidence for older events, including highstands around 50–95 ka, 100–200 ka, 170–250 ka, and ca. 700 ka (Kurth et al., 2010). Hydrothermal features include producing geothermal fields (Rye Patch, Jersey Valley, Dixie Valley, Fallon-Stillwater), hot springs, and fumaroles. The Dixie Valley geothermal field in particular is one of the largest and hottest non-magmatic geothermal system in the Basin and Range, generating ~62 MW from 248 °C hydrothermal fluids extracted from basin-bounding faults and associated fractures at 2-3 km depth (Blackwell et al., 2007). Several active hot springs in Dixie and Buena Vista valleys are associated with substantial travertine mounds that extend laterally over hundreds of meters and rise several meters above the local topography.

One particularly sizable, inactive travertine deposit blankets a large portion of canyon wall at Cottonwood Creek in the Stillwater Range adjacent to the hydrothermal field, and provides an interesting opportunity to investigate the source of the massive paleospring system. Located several kilometers inboard of the range front faults, the Cottonwood Canyon Travertine, or 'Dead Travertine' after Goff et al. (2002) and Lutz, et al., (2002), is a large, enigmatic Mid to Late Pleistocene deposit preserving some of the oldest travertine formations in Dixie Valley (Figure 1). The deposit extends several hundred meters above the canyon floor and drapes the northern wall of the canyon for several hundred meters along the base. Previous work has helped constrain the age, but the origin of this paleospring system is unclear: was there an active fault system providing deeply sourced hot fluids, or was fluid flow driven by wetter climatic conditions?

Here, we investigate the origin of these deposits using observations of the stratigraphic setting, travertine textures, conventional C and O isotope analyses, and carbonate clumped isotope ($T\Delta_{47}$) thermometry. We show that the composition of the source fluids responsible for the deposition of Cottonwood Travertine was likely similar to values observed locally in streams and seeps, and that the temperatures were not particularly hot. Based on the paleothermometry and previously reported age of the deposit, we favor an interpretation that suggests the main driving mechanism for the formation of the Cottonwood travertine was climatic, rather than hydrothermal or tectonic.

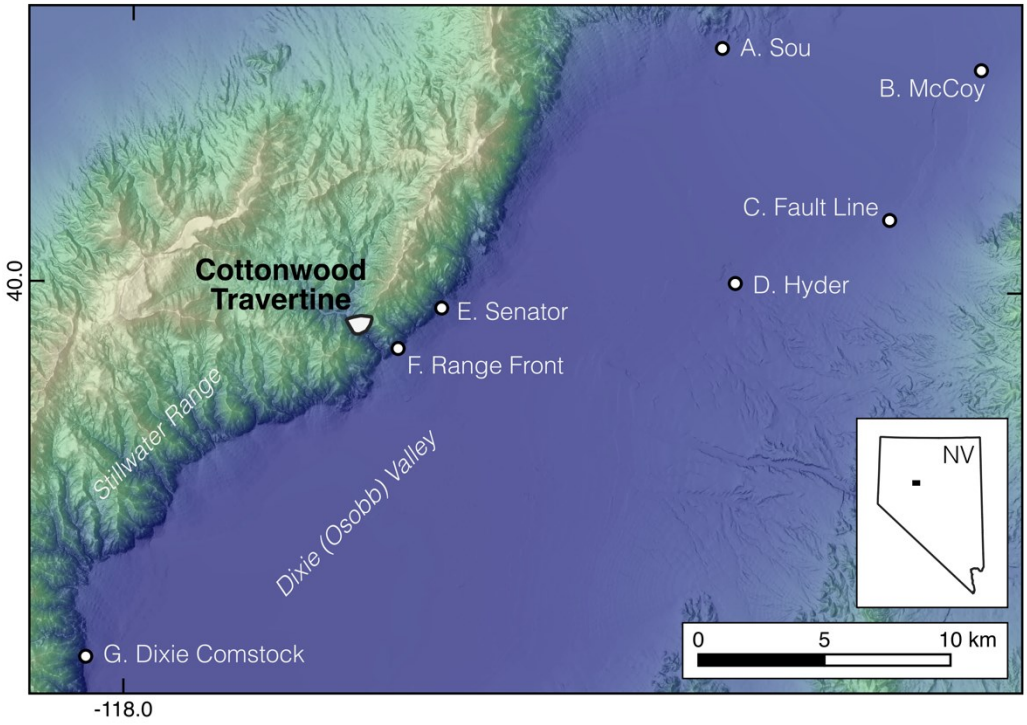

Figure 1. Cottonwood Canyon Travertine is located within the Stillwater Range, central Nevada. Detailed site topography is shown in Figure 2. Stable isotope values of calcite veins and travertine from sites A-G are included in Figure 5A.

2. GEOLOGY OF THE COTTONWOOD TRAVERTINE

The Cottonwood Travertine is one of the largest and oldest travertine deposits in the region. It is a sloping fan deposit covering 0.1 km^2 (24 acres) of a steep canyon wall 1.5-2 km west of the range front fault. The deposit originates as calcite-cemented gravels and terraces >130 m above the canyon floor and is 420 m wide along the base (Figure 2). Sloping mounds and steep fabric occur around 1430 m, with subtle mounds and onlapping travertine cropping out in several portions down the face of the apron (Figure 3A, 3B). The thickest preserved portion in the middle of the deposit is approximately 13 m thick (Figure 3B), but much of the canyon walls are only blanketed by a few meters or less of layered travertine. The deposit is deeply incised at the toe and by tributary canyons, revealing altered Jurassic basalt and carbonate-cemented quartz arenite of the Boyer Formation (Speed and Jones, 1969; Speed, 1976). The host rock is heavily fractured and hosts veins with different orientations, geometry, and textures. Goff et al. (2002) reported U-series and protactinium-231 ages of 182 ±4 ka and 161 ±15 ka, respectively, for calcite veins within the underlying Jurassic rock, and Dixon et al. (2003) reported a younger U/Th isochron age of 97 ka for layered travertine within the deposit. The specific locations and stratigraphic context of these samples is unclear.

Some portions of the deposit show evidence for dissolution and reprecipitation as vugs and stalactites, but no new travertine is currently forming, and no springs are clear candidates for the actual source of the material. Instead, low-flow, possibly ephemeral, muddy seeps occur at the toe of the deposit and in some portions of the deeper side canyons. The temperatures and $\delta^{18}O_W$ values of these seeps and other nearby creeks and well water are described in Table 1.

Table 1. Temperature and $\delta^{18}O_w$ values of modern water samples collected near Cottonwood Canyon travertine.

Site	Note	Temp. °C	$\delta^{18}O_W$ (‰ SMOW)	Source
Cottonwood Creek	canyon mouth, August 2022	28.6	-13.4	this study
Cottonwood Creek	Lower creek, May 1998	20.2	-14.6	Goff et al. 2002; 110
Cottonwood Creek	Middle creek, November 1997	14.0	-14.6	Goff et al. 2002; 58
Spring	"northeast margin, travertine deposit"	17.4	-14.9	Goff et al. 2002; DV97-56
Seep	At base of deposit	19.2	-15.0	Goff et al. 2002; DV99-209
Seep	At base of deposit	19-22	-13.8	Goff et al. 2002; DV99-210
Bolivia Well	Low flow artesian well near travertine	28.8	-14.8	Goff et al. 2002; DV97-57

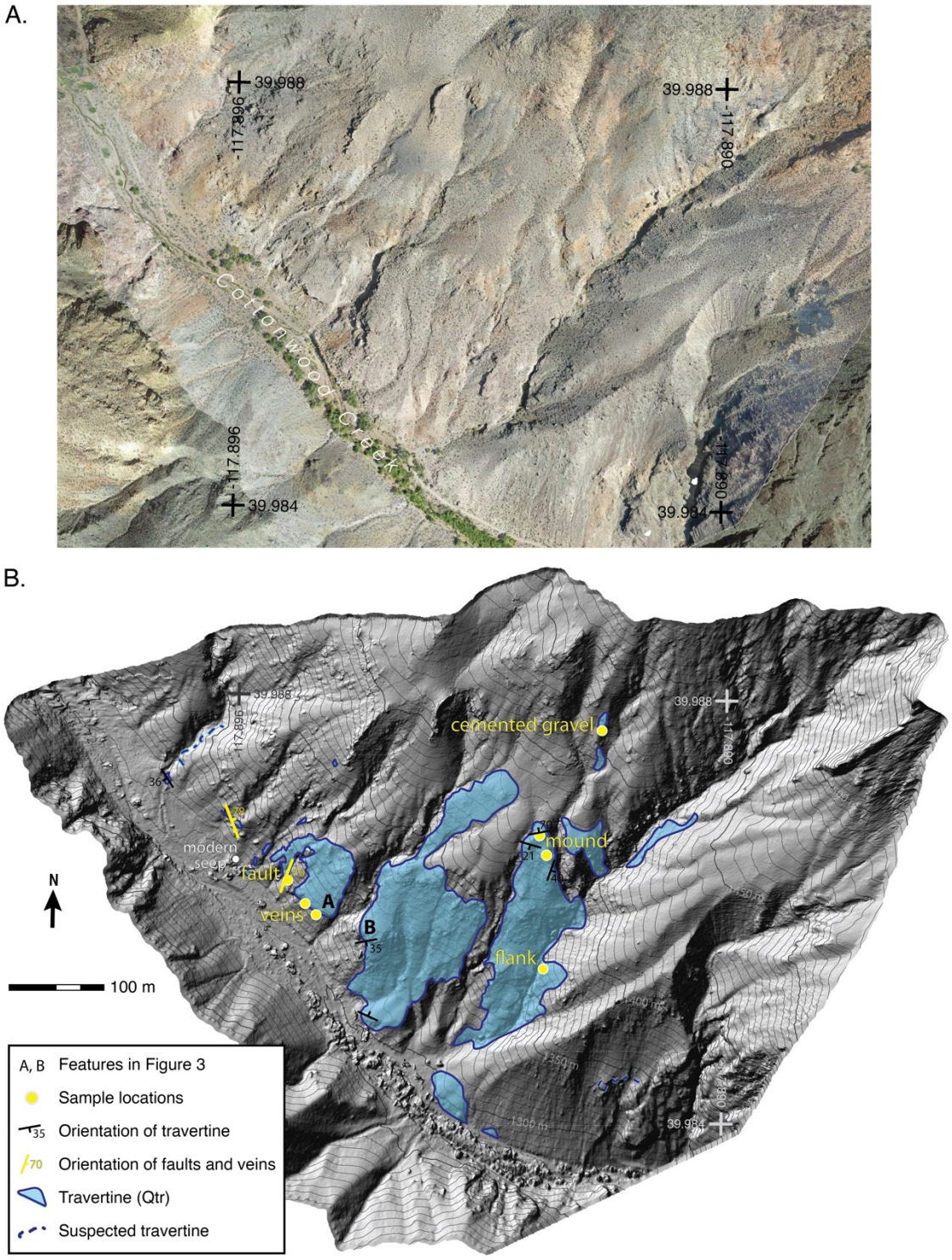

Figure 2. Cottonwood Canyon Travertine area with A) satellite imagery, orthorectified photomosaic, and B) shaded relief map. Heavily dissected travertine blankets altered Jurassic basalt and quartz arenite host rock on the northern side of Cottonwood Creek. Carbonate cemented gravels form ledges in alluvium above the deposit. The eastern and southeastern margin of the deposit include thick sequences of densely cemented gravel and travertine derived from the ridge to the southeast. A thick fault and vein arrays occur west of the main deposit. Samples are described in Table 2 and photographs from points A and B are shown in Figure 3. Basemaps from UAV-derived models described in Callahan et al. (2023) and available online at OpenTopography.

Figure 3. Outcrop images of the toe of the Cottonwood Canyon Travertine. A) View to northwest of a veneer of ~1 m of travertine (Qtr) on Jurassic Boyer Formation (Jb). B) View to southeast showing a several meter thick layered travertine deposit on Boyer Formation and altered basalt (Jvm). The southern toe of the travertine deposit, and a distant ridge of Jurassic gabbro (Jg) are visible beyond the thick travertine.

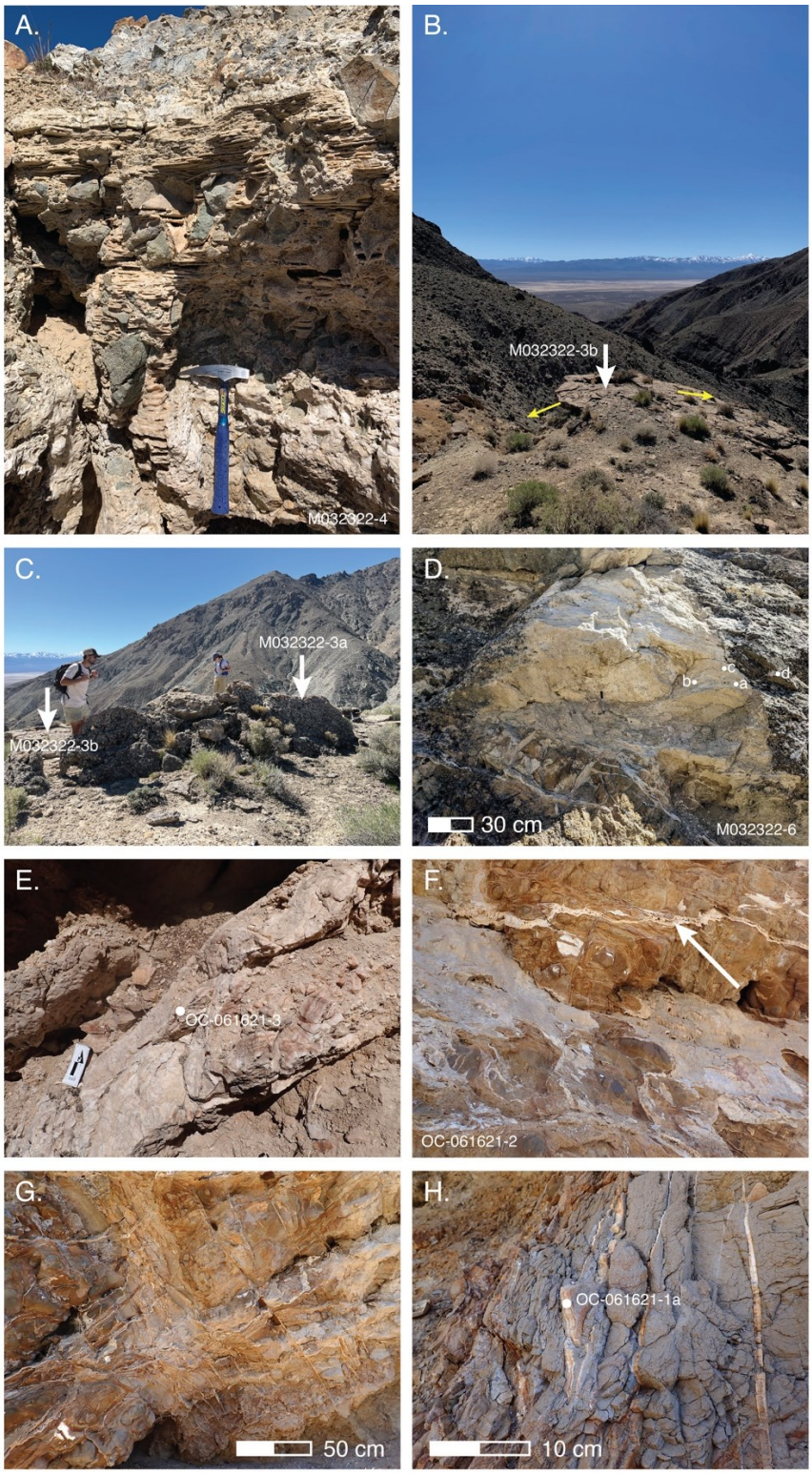

Figure 4. Sample settings at Cottonwood Travertine. Sample names included in each image and values reported in Table 2. Subsamples indicated by lowercase letters. A) Upper gravels. Hammer for scale. B and C) Upper mound sample area. White arrows point to sampled travertine locations. Yellow arrows indicate direction of assumed paleowater flow from slope of travertine layers. Subvertical fabric is encountered at M032322-3a. D) Sampled outcrop on the SE flank of the deposit with collection location of subsamples a-d. Subsample e is from veins below the layered travertine out of frame. E. Fault-vein on SW flank of the deposit. F) Thick, vuggy, low-angle vein below travertine at toe of deposit. Sampled area out of frame to the left. G and H) Altered Jurassic basalt and fibrous, subvertical veins beneath the toe of deposit.

3. FIELD AND GEOCHEMICAL METHODS

3.1 Mapping and Sample Collection

We mapped the extent of travertine and calcite-cemented alluvium, veins, and faults at the Cottonwood Canyon travertine deposit using digital mapping software and newly acquired basemaps with submeter resolution (Figure 2) (Callahan et al., 2023). We sampled centimeter wide subvertical veins in altered Jurassic rocks below the travertine, low angle veins with banded calcite below thick travertine sheets, a subvertical, decimeters-wide fault vein, mid-slope deposits, mounds at the top of the deposit, and cemented gravels above the main deposit for stable and clumped isotope analysis (Figure 4, Table 2).

3.2 Sample Preparation

Powders for isotopic analysis were prepared from raw materials in two ways. Powders collected in the field were drilled from the outcrop with a battery operated Dremel and ~1 mm wide carbide bit. Surface material was discarded, and material from the fresh, interior portions of the drill holes was collected in sample vials. Powders were also prepared from slabbed hand samples in the lab. Hand samples were slabbed with a water saw with single use distilled water. Bands of travertine were then drilled with a Dremel and carbide bit.

3.3 Stable Isotope Analytical Methods

Carbonate $\delta^{13}C$ and $\delta^{18}O_C$ measurements were conducted at the University of Washington IsoLab using a Kiel III Carbonate Device coupled to a Finnigan Delta Plus isotope ratio mass spectrometer with dual-inlet following the methods of Tobin et al. (2011). Measured values were normalized to the VPDB scale using a suite of internal reference materials that have been calibrated to international standards NBS19, NBS18, L-SVEC, and IAEA-603.

3.4 Clumped Isotope Analytical Methods

Carbonate clumped isotope (Δ_{47}) measurements, with concurrent $\delta^{13}C$ and $\delta^{18}O_C$ measurements, were conducted at the University of Washington IsoLab on selected samples using a custom automated sample preparation line and Thermo MAT 253 mass spectrometer following the methods of Burgener et al. (2016) and Schauer et al. (2016). Briefly, carbonate samples (6-8 mg) were digested in a common bath of phosphoric acid and the evolved CO_2 was cryogenically separated from water, isolated cryogenically, and transferred into a Pyrex break seal. Break seals containing CO_2 purified on the vacuum line are loaded into an automated 10-port tube cracker inlet system on the mass spectrometer. Δ_{47} values are calculated using established methods (Schauer et al., 2016) and are corrected to the carbon dioxide equilibrium scale (CDES) of Dennis et al. (2011) using CO_2 equilibrated with a suite of waters. Internal carbonate standards and ETH 1-4 were analyzed to track precision and accuracy in Δ_{47}, and to place $\delta^{13}C$ and $\delta^{18}O_W$ values on the VPDB scale. The temperature of formation is calculated from Δ_{47} after Anderson et al. (2021). The $\delta^{18}O_w$ values of paleospring water on the SMOW scale were derived from measured $\delta^{18}O_C$ and derived T Δ_{47} assuming equilibrium calcite precipitation using the equation of Kim and O'Neil (1997). For samples without clumped isotope T Δ_{47} measurements, estimated fluid $\delta^{18}O_W$ values of formation water were calculated from the range of T Δ_{47} values in nearby samples.

4. RESULTS

4.1 Mapping and Sample Collection

We identified several distinct textures, from platy, cement-supported colluvium in the upper reaches of the mapped extent, mounds and vertical fabrics resembling dissected orifices on the upper bench, thick, layered deposits down the flanks of the canyon walls, and faults and veins cutting the underlying Jurassic bedrock. The extent of travertine and sample locations are shown in Figure 2.

4.2 Stable Isotopes of Carbonate

Stable isotope analysis of 17 carbonate samples from Cottonwood Travertine revealed four groups with distinct properties: 1) calcite-cemented upper gravels, 2) top mound, 3) slope flanks, veins, and fault zone at the base, and 4) fibrous sub-travertine veins (Table 2). Samples from cements in the upper gravels had moderate $\delta^{13}C$ values (0.04 to 1.3‰ VPDB), and low $\delta^{18}O_C$ values (-18.4 to -16.5‰ VPDB). Samples from the mound on top of the main deposit had the highest $\delta^{13}C$ and $\delta^{18}O_C$ values (3.45 to 3.82‰ and -12.8 to -11.7‰ VPDB, respectively). Samples from the top mound, down the flank of the deposit, and from a lined fracture and cemented fault at the base of the deposit started with higher $\delta^{13}C$ values that generally decreased with elevation down the deposits. $\delta^{18}O_C$ values on the flank and base were between -15.9‰ and -14.5‰ VPDB and $\delta^{13}C$ values ranged -0.2 to 2.4 ‰ VPDB. The fibrous vein in altered Jurassic basalt associated with the Humboldt Igneous Group had the lowest $\delta^{13}C$ (-3.67 ±0.10‰ VPDB) and $\delta^{18}O_C$ (-29.42 ±0.11‰ VPDB) values of the samples.

4.3 Paleothermometry from Clumped Isotope of Carbonate

Clumped isotope thermometry of selected representative samples (n= 6) from the four groups also revealed differences depending on sample depositional setting (Table 2). The Δ_{47} value of 0.446 ±0.028‰ in the fibrous vein was the lowest of the analyzed material and corresponds to a calculated formation temperature of 93($^{+19}/_{-16}$)°C. Δ_{47} values from the top mound are 0.524 ±0.020 and 0.573 ±0.020‰, corresponding to temperatures of 24-32°C. Δ_{47} values from the lined fracture and cemented fault zone at the base of the deposit are 0.613 ±0.020 and 0.615 ±0.020‰, with calculated temperatures of 18 ($^{+6}/_{-6}$) and 19 ($^{+7}/_{-6}$)°C. The calcite-cemented gravels yielded $\delta^{18}O_C$ values as low as -18.39 ±0.12‰ (VPDB) and a Δ_{47} value of 0.524 ±0.020‰, corresponding to a temperature of 52 ($^{+9}/_{-8}$)°C.

4.4 Calculated $\delta^{18}O_W$ values of source water

Using measured values for $\delta^{18}O_C$ of the travertine, the range of calculated depositional temperatures from clumped isotopes, and equilibrium equations from Kim and O'Neil (1997), we inferred the $\delta^{18}O_W$ of the source fluids (Table 2). Carbonate cement in the upper gravels could form from source water with an $\delta^{18}O_W$ of around -11.1 ±1.5‰ SMOW, exceeding the average $\delta^{18}O_w$ value of modern waters by several permil (Table 1). Samples from the upper mound indicate a source fluid with an $\delta^{18}O_W$ between -9.0 and -9.6‰ SMOW, even more distinct from modern waters. $\delta^{18}O_C$ values in fractures and faults at the base of the deposit could originate from source waters with an $\delta^{18}O_W$ between -13.4 and -13.5‰ SMOW, nearly identical to modern waters. Conversely, assuming equilibrium with waters with similar isotopic composition as modern samples (δ^{18}Ow ~14.4‰ SMOW, Table 1), the formation temperature based on $\delta^{18}O_c$ values for samples from the flank and base of the deposit without clumped isotope thermometry (Table 2) is between 14-24 °C. The higher temperature and lower $\delta^{18}O_C$ of the fibrous calcite cement below the deposit require equilibrium conditions with waters at -16.1 ($^{+2.4}/_{-23}$)‰ SMOW which is lower than modern waters by several permil.

Table 2: Stable and Clumped Isotope Analysis of Cottonwood Canyon Travertine.

Sample Name*	Group	Material	Elev. (m)	Mean $\delta^{13}C$ (‰ VPDB)†	Mean $\delta^{18}O_C$ (‰ VPDB)†	n	Δ_{47} ‰‡	n	Temp. °C§	Calc. $\delta^{18}O_w$ (SMOW)**
M032322-4a	upper gravels	cement in upper gravels	1464	1.33 ±0.04	-18.39 ±0.12	3	0.524 ±0.020	2	52 ($^{+9}/_{-8}$)	-11.1 ±1.5
M032322-4b				0.04 ±0.04	-16.52 ±0.05	4				
M032322-3a	top mound	top mound	1432	3.82 ±0.14	-11.65 ±0.35	4	0.524 ±0.020	2	24 ($^{+7}/_{-6}$)	-9.6 ($^{+1.4}/_{-13}$)
M032322-3b				3.45 ±0.06	-12.76 ±0.28	4	0.573 ±0.020	2	32 ($^{+8}/_{-7}$)	-9.0 ±1.4
M032322-6a	flank and base	flank	1364	2.17 ±0.05	-15.16 ±0.10	3				
M032322-6b				1.85 ±0.05	-15.94 ±0.20	3				
M032322-6c				2.43 ±0.10	-14.85 ±0.15	3				
M032322-6d				1.77 ±0.06	-15.80 ±0.12	3				
M032322-6e		flank-vein		1.14 ±0.00	-14.52 ±0.06	2				
OC-061621-2a		lined fracture	1328	0.27 ±0.01	-14.45 ±0.05	2	0.613 ±0.020	2	19 ($^{+7}/_{-6}$)	-13.4 ±1.3
OC-061621-3a		fault zone	1327	0.99 ±0.01	-14.47 ±0.01	2	0.615 ±0.020	2	18 ($^{+6}/_{-6}$)	-13.5 ±1.3
OC-061621-3b				-0.13 ±0.02	-15.31 ±0.04	1				
OC-061621-3c				-0.21 ±0.04	-15.61 ±0.05	1				
OC-061621-3d				1.49 ±0.01	-14.82 ±0.03	1				
OC-061621-3e				0.33 ±0.03	-14.73 ±0.04	1				
OC-061621-3f				0.31 ±0.02	-14.77 ±0.04	1				
OC-061621-1a	sub-travertine	fibrous vein	1326	-3.67 ±0.10	-29.42 ±0.11	2	0.446 ±0.028	1	93 ($^{+19}/_{-16}$)	-16.1 ($^{+2.4}/_{-23}$)

* Subsample letter indicates samples from the same location, except for OC-061621-3* which were drilled from bands within the same sample. † Mean $\delta^{13}C$ and $\delta^{18}O$ from n replicates. Error is standard deviation, except for single replicates which show reported error. ‡ Showing standard error from laboratory standards for n replicates, which exceeds the standard deviation calculated from our replicates. § After Anderson et al., 2021. Range in temperatures is calculated from Δ_{47} standard error. ** After Kim and O'Neil (1997). Range of isotopic values from range of T Δ_{47}. Refer to Figure 4 for sample locations.

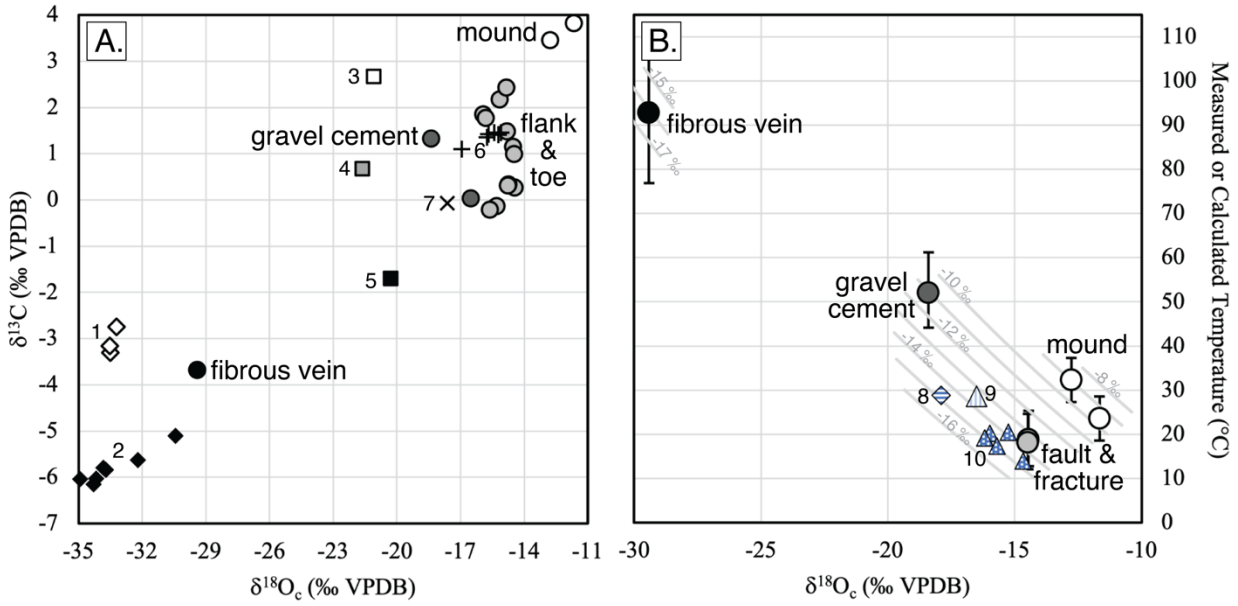

Figure 5. Results of stable (A) and clumped (B) isotope analysis. A. Stable isotope data from Cottonwood Travertine with representative examples from other Dixie Valley springs and fumaroles labeled 1-7: 1) Senator Fumaroles 2) Dixie Comstock epithermal deposit, 3) Sou Hot Springs, 4) Hyder Hot Springs, 5) McCoy Hot Springs, 6) Stillwater Range Front veins and travertine, and 7) Fault Line Springs. B. Temperature and $\delta^{18}O_C$ from samples with clumped isotope values and $\delta^{18}O_C$ values calculated for calcite in equilibrium with modern waters at 8) Bolivia Well, 9) Cottonwood Creek (this study), and 10) Cottonwood Creek and seeps from Goff et al. (2002) (Table 1). Grey lines indicate equilibrium composition for calcite deposited by waters with labeled $\delta^{18}O_W$ SMOW values at specified temperatures from Kim and O'Neil (1997).

5. DISCUSSION

Based on our field observations, stable isotope analysis, and clumped isotope thermometry, we suggest that the spring(s) that formed the Cottonwood Travertine were isotopically similar to modern local meteoric water (Table 1) and likely warm, but not near boiling as seen in other hot springs and fumaroles throughout Dixie Valley. All samples except for the fibrous vein are from shallow, Quaternary deposits based on their stratigraphic setting and textures. Most samples from the lower portion of the deposit could have formed in equilibrium with water that isotopically resembled local water at near-ambient temperatures (Tables 1 and 2, Figure 5B). And all samples except for the fibrous vein have higher $\delta^{18}O_c$ values than travertine from other local hot springs (Figure 5A). Unpublished data from Sou Hot Springs (<60°C), Hyder Hot Springs (<80°C), and McCoy Hot Springs (<50°C) contain $\delta^{18}O_c$ values below -20‰ VPDB. Instead, most samples from Cottonwood Travertine have $\delta^{18}O_c$ values closest to travertine from Fault Line Springs, where modern discharge temperature is <30°C.

Samples from the flanks of the deposit, vuggy, travertine lined veins near the toe of the deposit, and a decimeters-wide fault vein near the base all have a range of $\delta^{13}C$ values that broadly decrease with elevation, suggesting further distance from the spring source, and $\delta^{18}O_C$ values between -14.5 and -15.9‰ VPDB. Clumped isotope analysis on samples from two different locations on the flanks both suggest relatively low temperatures, ~20°C, and isotopic equilibrium with water that resembles modern waters (Tables 1, 2, Figure 5B).

Samples from the mound at the top of the deposit behave somewhat differently compared to the flanks and lead us to believe this area was likely the spring source (Figure 4B, 4C). These samples have unusually high $\delta^{18}O_C$ and $\delta^{13}C$ values compared to the rest of samples, and temperatures from clumped isotope analysis of ~24-32°C that are elevated from temperatures from the flank (Table 2, Figure 5A, 5B). The calculated $\delta^{18}O_W$ composition of the source water that would be in equilibrium with these values (>-10 ‰ SMOW), is much higher than most regional waters: local waters all have $\delta^{18}O_W$ values less than -13.4 ‰ SMOW (Table 1), and regional sources like Hyder Hot Springs and Sou Hot springs have values <-14 ‰ SMOW (Ingraham, 1982).

Instead of calling on an unusual source fluid composition, we infer kinetic effects caused by rapid degassing of CO_2 have resulted in disequilibrium conditions at the mound sites (Figure 4B, 4C). Based on the analysis of the residuals between observed and expected $\delta^{18}O_c$ and Δ_{47} described by Saenger et al. (2012) and Guo (2020), we suggest that off gassing of CO_2, consistent with rapid fluid ascent near the source, could explain the shift away from the isotopic composition of modern fluids and toward higher inferred $\delta^{18}O_w$ values (grey lines in Figure 5B). Off gassing is also consistent with the high $\delta^{13}C$ values at the mound site compared to the other samples (Gonfiantini et al., 1968). A similar but smaller effect is calculated for the calcite-cemented gravels above the main deposit (Figure 4A). These cements have lower $\delta^{18}O_C$ values and a calculated depositional temperature around 52°C (Figure 5A, 5B, Table 2). However, when compared to an expected source fluid closer to modern values (Table 1), they likewise plot in the field consistent with the degassing of CO_2. In both cases,

off gassing could result in an overestimation of the actual deposition temperature by 10-20°C. The interpretation of a cooler spring system is also consistent with higher $\delta^{18}O_C$ values compared to conditions at other known hot springs (Figure 5A).

The most extreme results that we encountered were obtained from veins cutting altered Jurassic basalt beneath the toe of the deposit. These veins appear distinct from the travertine deposit both texturally and geometrically (Figure 4G, 4H). They are also isotopically distinct from the travertine deposit: they have the lowest $\delta^{18}O_C$ and $\delta^{13}C$ values, differing from the average values of the rest of the samples by >10‰ and >3‰, respectively (Figure 5A). Compared to regional isotopic values for other travertine and carbonate veins shown (Figure 5A), this sample plots closer to samples from fumarole-related deposits at Senator Fumaroles (~100°C), or epithermal veins at Dixie Comstock (~150-200°C), both of which are also hosted in Jurassic clastic and mafic units (Vikre, 1993; Goff et al., 2002; Callahan, 2018, and unpublished data). The very low $\delta^{18}O_c$ values are consistent with the highest calculated $T\Delta_{47}$; near boiling at surface conditions (Figure 5B). Based on the isotopic and textural observations, we infer that many of these veins are unrelated to the hydrologic system that sourced the younger travertine deposits.

If the mounds are indeed the source area for Cottonwood Travertine, and the travertine composition represents the source fluid condition, and considering the Mid to Late Pleistocene age of veins and travertine deposits described by Goff et al. (2002) and Dixon et al. (2003), we suggest that wetter conditions during Marine Isotope Stage 6 are potentially responsible for formation of much of the travertine deposit in Cottonwood Canyon. MIS 6 is a period associated with the formation of large lakes throughout the western US (Smith, 1991; Lowenstein et al., 1999), and is also correlated with the formation of large travertine deposits in the Grand Canyon between 155-190 ka (Szabo, 1990), which brackets the U-series ages of 182 ±4 ka and 161 ±15 ka presented by Goff et al. (2002). The preliminary age of 97 ka from Cottonwood Travertine presented by Dixon et al. (2003) is likewise similar in age to other travertine deposits in the Grand Canyon described by Szabo (1990). Unfortunately, without knowing the stratigraphic, structural, and diagenetic context of any of the previously reported ages of the Cottonwood deposit it is difficult to place the system into a specific paleoclimate context. However, we do think that a wetter climate likely played an essential role in the formation of this warm-spring deposit, and are less in favor of a young, near boiling system as may be inferred by our highest calculated temperature. These interpretations assume the mounds at the top of the deposit (Figure 4A, 4B, 4C) are the original spring source. However, it is possible we did not collect samples representing elevated temperatures indicating a depositional hot spring because the true spring source remains undiscovered, and we invite further field investigations.

6. CONCLUSION

We presented results of geologic and stable isotope ($\delta^{13}C$, $\delta^{18}O_C$, Δ_{47}) analyses of an unusually large, Mid to Late Pleistocene, intramountain travertine deposit in Cottonwood Canyon, Stillwater Range, Nevada. The inferred $\delta^{18}O_w$ composition of source water in equilibrium with the deposit is similar to isotopic values of cold springs, seeps, creeks, and warm wells observed locally today. Clumped isotope temperatures for all samples range from ~18 to 93 °C; however, the hottest temperature is isotopically and texturally distinct from the rest of the samples, and we suggest may be unrelated to the hydrologic system that generated the deposit. The remaining temperature calculations suggest the source fluids were not particularly hot and, based on the paleothermometry and previously reported age of the deposits, we favor an interpretation that suggests a CO_2-rich warm-spring outflow from relict mounds observed on the upper bench. We suggest that the main driver of deposition at this site was a wetter climate condition in the mid to Late Pleistocene and not a distinct period of hydrothermal or tectonic activity.

ACKNOWLEDGEMENTS

This work was supported by NSF EAR Tectonics Award #2040716 to OAC, JGC, and KWH and a grant from the Quaternary Research Center to OAC and JGC. Funds from the NSF GeoALLIES program (Award #2037292) supported undergraduate fieldwork. AJ was supported by the University of Washington Department Earth and Space Sciences Afton Woolley Crooks & James William Crooks Endowed Scholarship in Geological Sciences, the Joseph A. Vance Endowed Student Support Fund and University of Washington Douglas E. Merrill Prize for Excellence. We would also like to thank Fraser Goff and Gabe Plank for discussions about this site.

REFERENCES

Adams, K. D., Goebel, T., Graf, K., Smith, G. M., Camp, A. J., Briggs, R. W., and Rhode, D.: Late Pleistocene and Early Holocene Lake-Level Fluctuations in the Lahontan Basin, Nevada: Implications for the Distribution of Archaeological Sites, Geoarchaeology, 23(5), (2008), 608-643. 10.1002/gea.20237

Anderson, N. T., Kelson, J. R., Kele, S., Daëron, M., Bonifacie, M., Horita, J., Mackey, T. J., John, C. M., Kluge, T., Petschnig, P., Jost, A. B., Huntington, K. W., Bernasconi, S. M., and Bergmann, K. D.: A Unified Clumped Isotope Thermometer Calibration (0.5–1,100°C) Using Carbonate-Based Standardization, *Geophysical Research Letters*, *48*(7), (2021). https://doi.org/10.1029/2020gl092069

Benson, L.:Factors Affecting ^{14}C Ages of Lacustrine Carbonates: Timing and duration of the Last Highstand Lake in the Lahontan Basin, Quaternary Research, 39, (1993), 163-174.

Blackwell, D. D., Smith, R. P., and Richards, M. C.: Exploration and Development at Dixie Valley, Nevada: Summary of DOE Studies, Proceedings, 32nd Workshop on Geothermal Reservoir Engineering, Stanford University, Stanford, CA, (2007).

Burgener, L., Huntington, K. W., Hoke, G. D., Schauer, A., Ringham, M. C., Latorre, C., and Díaz, F. P.: Variations in Soil Carbonate Formation and Seasonal Bias Over >4 km of Relief in the Western Andes (30°S) Revealed by Clumped Isotope Thermometry, Earth and Planetary Science Letters, 441, (2016), 188–199. https://doi.org/10.1016/j.epsl.2016.02.033

Callahan, O. A.: Interactions Between Chemical Alteration, Fracture Mechanics, and Fluid Flow in Hydrothermal Systems, PhD, The University of Texas at Austin, (2018).

Callahan, O. A., Brigham, C. A. P., Heitmann, E., Sullivan, E., Jackson, A., Mat, S. R., Mudambi, J., Osako, J., Needle, M., Huntington, K., Crider, J. G.: High-Resolution Structure-from-Motion Models of Hydrothermal Sites in the Central Nevada Seismic Belt: Applications in Tectonic, Climate, and Hydrothermal Investigations, Proceedings, 48th Workshop on Geothermal Reservoir Engineering, Stanford University, Stanford, CA, (2023).

Caskey, S. J., and Ramelli, A. R.: Tectonic Displacement and Far-Field Isostatic Flexure of Pluvial Lake Shorelines, Dixie Valley, Nevada, Journal of Geodynamics, 38(2), (2004), 131-145. https://doi.org/10.1016/j.jog.2004.06.001

Dennis, K. J., Affek, H. P., Passey, B. H., Schrag, D. P., Eiler, J. M.: Defining an Absolute Reference Frame for "Clumped" Isotope Studies of CO_2, Geochimica et Cosmochimica Acta, 75, (2011), 7117–7131. https://doi.org/10.1016/j.gca.2011.09.025

Dilek, Y., and Moores, E. M.: Geology of the Humboldt Igneous Complex, Nevada, and Tectonic Implications for the Jurassic Magmatism in the Cordilleran Orogen, in D. M. Miller & C. Busby (Eds.), Jurassic Magmatism and Tectonics of the North American Cordillera, Geological Society of America Special Paper 299, (1995). https://www.doi.org/10.1130/SPE299-p229

Dixon, E.T., Murrell, M., Goff, F., and Goldstein, S.: Uranium-Series Geochronology of Hydrothermal Deposits, Dixie Valley, Nevada, *EOS, Transactions American Geophysical Union*, Fall Meeting, San Francisco (Dec. 8-12), 84 (46), (2003).

Goff, F., Bergfeld, D., Janik, C. J., Counce, D., and Murrel, M.: Geochemical Data on Waters, Gases, Scales, and Rocks from the Dixie Valley Region, Nevada (1996-1999), LA-13972-MS, (2002). https://www.osti.gov/servlets/purl/894412

Gonfiantini, R., Panichi, C., and Tongiori, E.: Isotopic Disequilibrium in Travertine Deposition, Earth and Planetary Science Letters, 5, (1968), 51-58.

Guo, W.: Kinetic Clumped Isotope Fractionation in the DIC-H_2O-CO_2 System: Patterns, Controls, and Implications, Geochimica et Cosmochimica Acta, 268, (2020), 230-257. https://doi.org/10.1016/j.gca.2019.07.055

Ingraham, N. L.: Environmental Isotope Hydrology of the Dixie Valley Geothermal System, Dixie Valley, Nevada, MS, University of Nevada, Reno, (1982).

Kele, S., Bernasconi, S. M., Kluge, T., John, C. M., Millan, I. M., Meckler, A. N., et al.: Clumped Isotope Geochemistry of Travertine Carbonates in the 22-95°C Temperature Range. Geochimica et Cosmochimica Acta, 70, (2006), 1439-1456.

Kim, S.-T., and O'Neil, J. R.: Equilibrium and Nonequilibrium Oxygen Isotope Effects in Synthetic Carbonates, Geochimica et Cosmochimica Acta, 61, (1997), 3461–3475. https://doi.org/10.1016/S0016-7037(97)00169-5

Kurth, G., Phillips, F. M., Reheis, M. C., Redwine, J. L., and Paces, J. B.: Cosmogenic Nuclide and Uranium-Series Dating of Old, High Shorelines in the Western Great Basin, USA, Geological Society of America Bulletin, 123(3-4), (2010), 744-768. https://doi.org/10.1130/B30010.1

Lin, J. C. (1998). A Reassessment of the U-Th and ^{14}C Ages for Late-Glacial High-Frequency Hydrologic Events at Searles Lake, California, Quaternary Research, 49, (1998), 11-23.

Lowenstein, T. K., Li, J., Brown, C., Roberts, S. M., Ku, T.-L., Luo, S., and Yang, W.:, 200 k.y. Paleoclimate Record from Death Valley Salt Core, Geology, 27, (1999), 3-6.

Lutz, S. J., Caskey, S. J., Mildenhall, D. D., Browne, P. R. L., and Johnson, S. D.: Dating Sinter Deposits in Northern Dixie Valley, Nevada - The Paleoseismic Record and Implications for the Dixie Valley Geothermal System, Proceedings, 27th Workshop on Geothermal Reservoir Engineering, Stanford University, Stanford, CA, (2002).

Saenger, C., Affek, H. P., Felis, T., Thiagarajan, N., Lough, J. M., and Holcomb, M.: Carbonate Clumped Isotope Variability in Shallow Water Corals: Temperature Dependence and Growth-Related Vital Effects, Geochimica et Cosmochimica Acta, 99, (2012), 224-242. https://doi.org/10.1016/j.gca.2012.09.035

Schauer, A. J., Kelson, J., Saenger, C., and Huntington, K. W.: Choice of ^{17}O Correction Affects Clumped Isotope (Δ_{47}) Values of CO_2 Measured with Mass Spectrometry, Rapid Communications in Mass Spectrometry, 30, (2016), 2607–2616. https://doi.org/10.1002/rcm.7743

Smith, G. I.: Stratigraphy and Chronology of Quaternary-Age Lacustrine Deposits, *in*: Morrison, R.B. (Ed.): Quaternary Nonglacial Geology: Conterminous U.S., Geological Society of America, Boulder, Colorado, (1991), 339–352.

Speed, R. C. (Cartographer): Geologic Map of the Humboldt Lopolith and Surrounding Terrane, Nevada, (1976).

Speed, R. C., and Jones, T. A.: Synorogenic Quartz Sandstone in the Jurassic Mobile Belt of Western Nevada: Boyer Ranch Formation, Geological Society of America Bulletin, 80, (1969), 2551-2584.

Szabo, B. J.: Age of Travertine Deposits in Eastern Grand Canyon National Park, Arizona, Quaternary Research, 34, (1990), 24-32.

Thompson, G. A., and Burke, D. B.: Rate and Direction of Spreading in Dixie Valley, Basin and Range Province, Nevada. Geological Society of America Bulletin, 84(2), (1973), 627-632. https://www.doi.org/10.1130/0016-7606(1973)84<627:radosi>2.0.co;2

Tobin, T.S., Schauer, A.J., and Lewarch, E.: Alteration of Micromilled Carbonate $\delta^{18}O$ During Kiel Device Analysis, Rapid Commun. Mass Spectrom, 25, (2011), 2149–2152. http://dx. doi.org/10.1002/rcm.5093

Vikre, P. G.: Gold Mineralization and Fault Evolution at the Dixie Comstock Mine, Churchill County, Nevada, Economic Geology, 89(4), (1993), 707-719. https://doi.org/10.2113/gsecongeo.89.4.707

Winograd, I. J., Coplen, T. B., Landwehr, J. M., Riggs, A. C., Ludwig, K. R., Szabo, B. J., et al.: Continuous 500,000-year Climate Record from Vein Calcite in Devils Hole, Nevada, Science, 258(5080), (1992), 255-260.